crystals

MDPI

*Review*

# Suspended 2D Materials: A Short Review

**Yunyun Dai [1,2,†], Tongtong Xue [3,†], Xu Han [1], Xinyu Huang [1], Decheng Zhang [1], Mengting Huang [1], Jiahao Yan [1], Jinghan Zhao [3], Vijay Laxmi [1], Liwei Liu [1], Xiaolong Xu [1], Yeliang Wang [1,*] and Yuan Huang [1,2,4,*]**

1 MIIT Key Laboratory for Low-Dimensional Quantum Structure and Devices, School of Integrated Circuits and Electronics, Beijing Institute of Technology, Beijing 100081, China; yunyundai@bit.edu.cn (Y.D.); hanxu0037@bit.edu.cn (X.H.); xinyuhuang@bit.edu.cn (X.H.); 3220210693@bit.edu.cn (D.Z.); huangmengting@bit.edu.cn (M.H.); yanjh@bit.edu.cn (J.Y.); vijaylaxmigupta90@gmail.com (V.L.); liwei.liu@bit.edu.cn (L.L.); xuxiaolong@bit.edu.cn (X.X.)
2 Advanced Research Institute of Multidisciplinary Sciences, Beijing Institute of Technology, Beijing 100081, China
3 Department of Physics, Beijing Institute of Technology, Beijing 100081, China; 3120221982@bit.edu.cn (T.X.); 3120221984@bit.edu.cn (J.Z.)
4 BIT Chongqing Institute of Microelectronics and Microsystems, Chongqing 401332, China
* Correspondence: yeliang.wang@bit.edu.cn (Y.W.); yhuang@bit.edu.cn (Y.H.)
† The authors contribute equally to this work.

**Abstract:** In recent years, there has been a growing fascination with suspended two-dimensional (2D) materials, owing to their excellent mechanical, optical, and electronic characteristics. This surge of interest stems from the remarkable properties exhibited by these materials when they are isolated in a two-dimensional counterpart. Nanofabrication technologies provide a new platform to further explore the properties of 2D materials by suspending them to reduce the influence of substrates. In recent years, many scientists have discovered the feasibility of using suspended membranes of 2D materials in various fields, including optoelectronics and photonics. This review summarizes the recent progress in the fabrication, characterization, and applications of suspended 2D materials, focusing on critical properties such as optical and electronic properties, strain engineering, and thermal properties. This area has the potential to lead to new technologies and applications in a wide range of innovative fields.

**Keywords:** suspended; two-dimensional materials; nanofabrication; light enhancement; superconducting



**Citation:** Dai, Y.; Xue, T.; Han, X.; Huang, X.; Zhang, D.; Huang, M.; Yan, J.; Zhao, J.; Laxmi, V.; Liu, L.; et al. Suspended 2D Materials: A Short Review. *Crystals* **2023**, *13*, 1337. https://doi.org/10.3390/cryst13091337

Academic Editor: Thorsten Hesjedal

Received: 6 June 2023
Revised: 24 August 2023
Accepted: 29 August 2023
Published: 1 September 2023



## 1. Introduction

Two-dimensional (2D) materials, such as graphene, transition metal dichalcogenides (TMDs), and black phosphorus, have attracted significant attention in recent years due to their promising properties and potential applications in electronic, photonic, and mechanical devices [1–12]. In addition, 2D materials have vast prospects in applications such as sensing [13,14], energy storage, and conversion [15–18]. However, due to their atomic thickness, the properties of 2D materials can be significantly influenced by the surrounding environment, including the substrate [19–21], applied strain [22,23], and other external factors. The interaction between the 2D material and the substrate leads to undesirable effects such as undesirable doping [24–26], quenching [27–30], and scattering [31], which can obscure or modify the optical responses of the material and, ultimately, the whole device's performance. One way to exploit these intrinsic properties is to suspend the 2D materials, allowing one to have greater control over the surrounding environment [32].

Suspended 2D materials have been gaining significant attention to eliminate substrate-induced perturbations [4,33–38]. In contrast to supported 2D materials [19], suspended 2D materials are not influenced by the substrate, which induces undesirable doping [24–26] or scattering, not only enabling the study of intrinsic properties [39], but also providing more degrees of freedom in device design [40]. Suspended 2D materials have recently shown great potential applications in high-performance devices, such as suspended

$MoS_2$ transistors with high on/off ratios [41,42] and graphene FET with excellent mobility (250,000 $cm^2/Vs$) [43]. Moreover, the suspended structure, acting as a cavity, enhances the signals, such as the enhanced light emission from a suspended monolayer $WS_2$ in a Fabry–Pérot microcavity [44]. Therefore, suspended 2D materials have emerged as a solution to overcome the challenges posed by substrates, providing valuable insights for researchers seeking to investigate and harness the unique optical, mechanical, and other various properties of 2D materials.

Another approach to eliminate the influence of the substrate is to encapsulate 2D materials [45–49]. A notable case is exemplified by the work of Sattari-Esfahlan et al., who fabricated a graphene field-effect transistor (FET) by interposing graphene amid two layers of amorphous boron nitride [46]. In comparison with conventional graphene FETs, with a mobility within the range of 2000–15,000 $cm^2/Vs$, the encapsulated graphene FET demonstrates higher mobility (17,941 $cm^2/Vs$). The encapsulation provides a protective layer that shields the 2D material from external factors such as moisture, oxygen, and contaminants, leading to improved material stability and decreased degradation. However, the encapsulation layers hinder the interaction between the 2D material and the surrounding environment, reducing the sensitivity or response of the material to certain stimuli. Additionally, encapsulated 2D materials are constrained by the substrate or the encapsulation materials. Therefore, compared with encapsulated 2D materials, suspended 2D materials, which are more sensitive to the environment and have greater flexibility and elasticity, enable more applications, such as sensors and flexible electronics.

In this review, we explore the concept of suspending 2D materials, wherein the material is isolated from the substrate using various methods such as transfer techniques and nano/microfabrication methods. The past decade has seen significant progress in the fabrication, [50] characterization [32,51], and application [50,52] of suspended 2D materials. We discuss the advantages of such suspended configurations, including eliminating substrate effects on the optical properties of the 2D material. Furthermore, we delve into the experimental techniques used to create suspended 2D material structures [53–56], including membrane fabrication, cantilever-based designs, and nanomanipulation techniques. We highlight the importance of achieving a stable and controlled suspension and the challenges involved in maintaining the suspended material's structural integrity.

Additionally, we showcase the distinct optical properties, electronic properties, and mechanical flexibility of suspended 2D materials investigated in various research studies [39,40,53,57–59]. These properties include enhanced light–matter interactions, increased photoluminescence (PL) emission, strain engineering, high mobility, and tunable visual responses. We provide examples of specific 2D materials, such as graphene and TMDCs, where suspended configurations have enabled the characterization and exploitation of their unique properties. Here, we emphasize the significance of suspended 2D materials in overcoming substrate challenges for exploring the unique properties of these materials. We offer insights into suspended configurations' experimental techniques, advantages, and limitations. The findings presented here will serve as a valuable resource for researchers aiming to harness the full potential of 2D materials in various applications, including FETs [41,60,61], logic gates [62,63], photodetectors [64–68], resonators [69–72], and sensors [73–78].

## 2. Fabrication Techniques of Suspended 2D Materials

Numerous methods of preparing 2D materials have been developed in prior research, including mechanical exfoliation [50], chemical vapor deposition [79], liquid-phase exfoliation [80], and solution-based approaches [81], among others. In recent years, additional innovative preparation techniques have emerged, such as the vacuum-kinetic spray process [82] and controlled gas exfoliation [83]. Additionally, binder-free direct coating techniques [84–86] for the large-scale production of 2D materials have gained significant importance in the room-temperature fabrication of functional devices for commercial applications. While fabricating 2D materials on substrates is well-established, the preparation of suspended 2D materials poses more significant challenges. Researchers have developed

various methods to obtain suspended 2D materials [53–56]. Most of the current fabrication methods rely on the transferring of 2D materials onto pre-fabricated suspended structures [32]. This method involves the transfer of 2D materials from their original substrate onto a pre-fabricated suspended structure, such as a structured $SiO_2$ substrate or polymer membrane. Additionally, a direct synthesis method can be employed to produce suspended 2D materials [87]. This approach enables the rapid and large-scale production of suspended 2D materials.

Recently, Huang et al. proposed an efficient method for the fabrication of suspended monolayers of 2D materials, as illustrated in Figure 1 [32]. The researchers utilized a microfabrication process to create a suspended bridge structure, enabling the transfer of the 2D material onto the patterned substrate. To prepare the patterned substrate, lithographic techniques and plasma processing with $SF_6$ were used. These treatments were crucial, as the interaction between the 2D materials and the substrates plays a pivotal role in the subsequent exfoliation process, enabling proper adhesion and, thus, successful transfer of the 2D materials onto the prepared substrate. For materials such as graphene and cuprate superconductors (e.g., Bi2212 or $Bi_2Sr_2CuO_6$), the substrates proved quite useful in effectively producing large-area 2D flakes through the use of oxygen plasma processing [88]. Freshly cleaved graphite tape was carefully placed onto the treated substrate and heated at 100 °C for 1 min. Upon cooling, the tape was peeled off, resulting in high-quality suspended graphene flakes. However, for materials like MDC (metal dichalcogenides) or BP (black phosphorus), where the interaction with the substrate was not strong enough to ensure efficient exfoliation, the authors adopted a different strategy. They coated the patterned substrate with Au/Ti (gold/titanium) before placing the freshly cleaved crystal [50,89,90]. This approach proved effective for preparing dozens of 2D materials.

The fabricated suspended monolayers displayed various geometrical structures such as rectangles, Hall bars, and circles (Figure 1b–d). Additionally, irregular shapes, including Chinese zodiac sign structures, were successfully achieved (Figure 1f). The method was shown to be effective in producing suspended monolayers with excellent optical (Figure 1e) and electronic properties, making them ideal for various applications such as nanoelectronics, photonics, and biosensing.

In addition to the transfer method, other methods have been developed for preparing suspended 2D materials, such as the use of bubbles [91–96]. Luo et al. reported on the fabrication of bubbles by utilizing the interaction between $MoS_2$, the substrate, and gas molecules (Figure 2). Initially, the $SiO_2$/Si substrate is exposed to oxygen plasma, which effectively removes adsorbates from the surface. Then, a tape with thin $MoS_2$ is applied to the treated substrate. The substrate and the $MoS_2$-loaded tape are heated for approximately 1 to 2 min at a temperature of around 110 °C in ambient air. During this heating process, the interface between the $MoS_2$ and the substrate acts as a trap for small gas molecules in the surrounding air. As the substrate is heated on a hot plate, these trapped gas molecules accumulate and form bubbles. After the sample has cooled down to room temperature, the adhesive tape is removed, leaving bubbles between the $MoS_2$ and the substrate (Figure 2a). Large $MoS_2$ bubbles with diameters up to 60 μm can be obtained (Figure 2b). It is worth pointing out that the shape of these $MoS_2$ bubbles can stay intact after one year. The authors demonstrated that the strain induced by the bubble led to the simultaneous generation of both direct and indirect PL (Figure 2c), which has implications for optoelectronic applications.

Despite recent advancements [97–101], the development of efficient and reproducible fabrication methods for high-quality suspended 2D materials continues to pose a significant challenge. One major challenge lies in achieving a stable, undamaged, and controlled suspension while eliminating the supporting substrate and maintaining the integrity of the thin material. The etching or exfoliation processes can introduce defects and contamination, potentially leading to non-uniformity and unintended doping of the 2D materials [102–106]. Additionally, the fabrication of suspended 2D materials at a large scale remains a challenge due to several factors. First, the scalability of suspended 2D materials starts with the

synthesis techniques. Conventional methods, such as mechanical exfoliation or chemical vapor deposition, are limited in terms of producing large-area or high-quality materials. Developing scalable synthesis methods that can produce large quantities of high-quality 2D materials is essential. After synthesis, the 2D materials need to be transferred onto target substrates. The transfer techniques should ensure the material uniformity on a large scale and minimize defects introduced during the process. Advances in synthesis techniques, transfer methods, material stability, and device integration are being pursued to enable the large-scale production of suspended 2D materials. Addressing these challenges is of significant importance for advancing the fabrication techniques required for suspended 2D materials, thereby enabling their application in various domains such as nanoelectronics and optoelectronics.

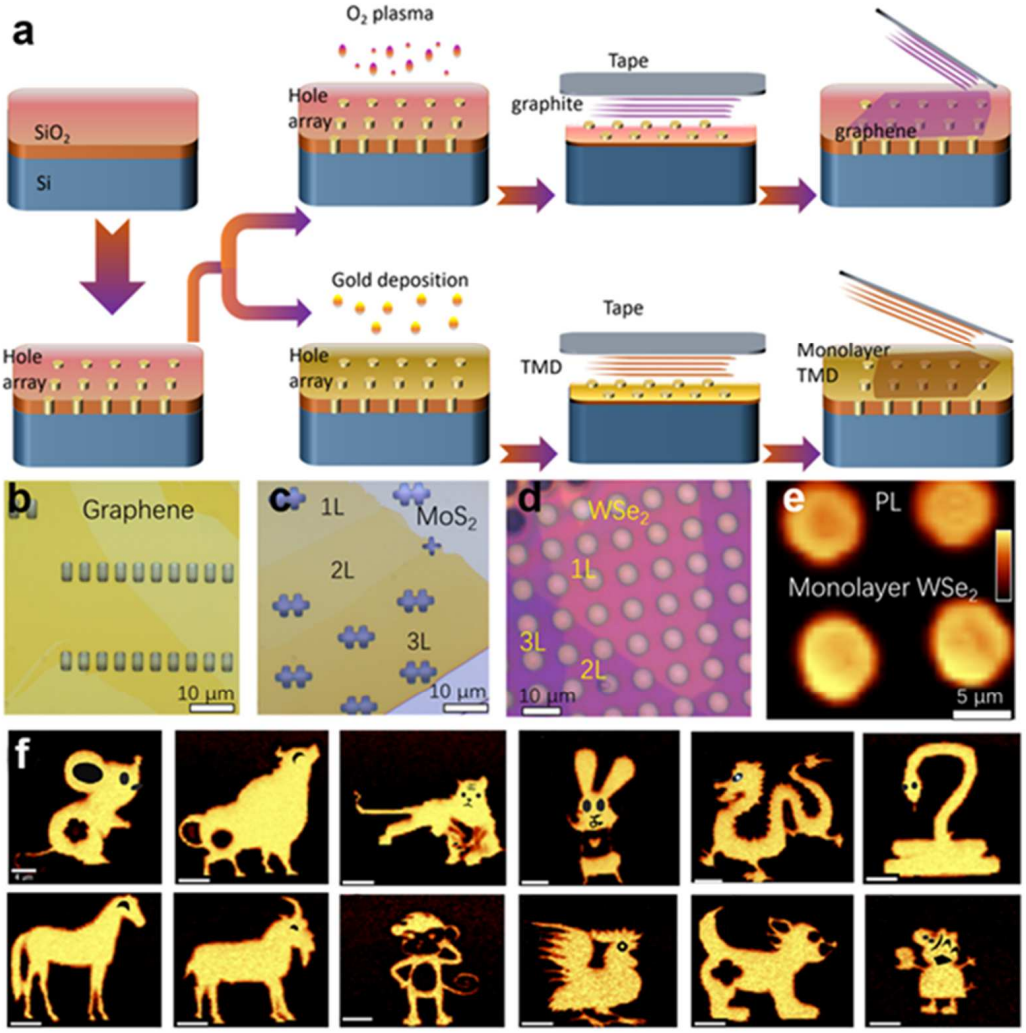


**Figure 1.** Fabrication process and optical characterization of the suspended 2D materials. (**a**) Illustrations of the fabrication process for suspended 2D materials [32]. (**b**–**d**) Photographs of exfoliated graphene, $MoS_2$, and $WSe_2$ on structured substrates. (**e**) PL mapping of suspended monolayer TMCs on the hole substrate. (**f**) The PL mapping images reveal Chinese zodiac signs due to the PL enhancement at the suspended regions. The scale bar is 4 μm.

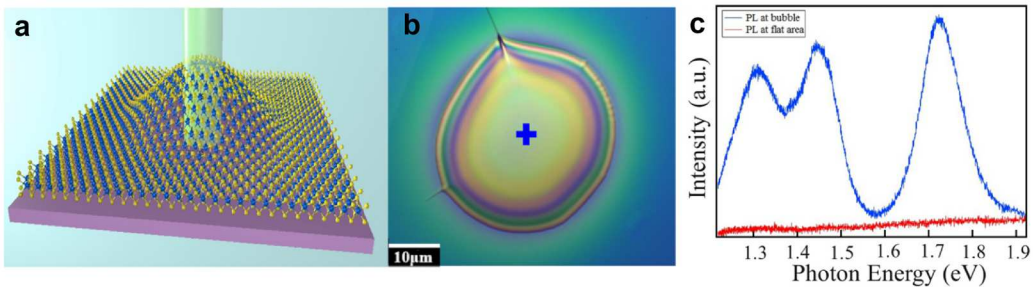


**Figure 2.** The fabrication process and the characterization of suspended 2D materials by making bubbles. (**a**) Schematic diagram of a $MoS_2$ bubble on Si substrate with a 532 nm laser beam irradiating on the exfoliated $MoS_2$ flake. (**b**) The optical image of a $MoS_2$ bubble on $SiO_2$/Si substrate, which exhibits Newton Rings due to the light interference. (**c**) PL measurements were taken from two distinct regions: the $MoS_2$ bubble center, represented by the red curve (marked by the red cross in (**b**)), and the flat region, indicated by the blue curve (marked by the blue cross in (**b**)) [91]. Reprinted with permission from Ref. [91]. Copyright 2020, American Physical Society.

## 3. The Properties of Suspended 2D Materials

Two-dimensional materials have unique and exceptional optical, excitonic, mechanical, and electronic properties that are of great interest for applications in next-generation photonics, electronics, and optoelectronic devices [1–3,11]. However, in supported 2D materials, the substrate induces additional strain or doping, which affects the accurate measurement of the intrinsic properties of the 2D materials [21,23,107–111]. The influence of the underlying $SiO_2$ substrate on 2D materials, for instance, was thoroughly investigated by Shi et al. using techniques such as electrostatic force microscopy, Raman spectroscopy, and electrical characterization. Their findings revealed that the contact potential difference between $SiO_2$ substrates and single-layer graphene determines the direction of the dipole formed at the interface, resulting in the doping of graphene [112]. Additionally, supported 2D materials are strongly affected by the substrates due to moving carriers or trapped charges at the interface [19]. Devices fabricated on $SiO_2$/Si substrate, for example, strongly disperse graphene due to the presence of charge traps [113]. Therefore, the suspended structure allows for improved access to the intrinsic electronic and optical properties of the material, which can be studied using various techniques such as Raman spectroscopy, STM, and PL spectroscopy.

In comparison with 2D materials deposited on a substrate, the characterization of the intrinsic electronic properties of suspended 2D materials is more accurate, as it eliminates any influence or background signals caused by the substrate. Significant advancements have been made in understanding graphene's carrier mobility through studies on the transport properties of suspended graphene. Notably, the mobility of the suspended graphene exhibited a ten-fold increase compared with that observed in conventional devices fabricated with substrates. Moreover, the utilization of in situ current annealing by Li et al. resulted in a substantial enhancement of graphene's transport properties. This improvement was demonstrated by the electrical characterizations of suspended graphene devices in a vacuum. Specifically, the carrier mobility increases as the width of the Dirac peak decreases [114]. Additionally, suspended 2D materials offer an ideal platform for investigating the quantum Hall effect. These materials possess uniform quality, relatively flat surfaces, an absence of defects or impurities, and favorable electrical characteristics, making them perfect candidates for studying the underlying physics of the quantum Hall effect [115–117]. Furthermore, the preparation methods employed for suspending 2D materials in this work have the potential to produce large-area, high-quality materials, which is crucial for enabling large-scale applications involving the quantum Hall effect. Therefore, the exploration of the quantum Hall effect using suspended 2D materials presents significant potential and promising prospects for practical applications.

The suspended structure presents a promising approach for enhancing the optical characteristics of 2D materials, opening up potential applications in diverse fields such as optoelectronics, nonlinear optics, and quantum information processing. A notable example of this potential was demonstrated in the research conducted by Shi et al. In their study, significant amplification and controlled second harmonic generation (SHG) were observed from suspended single-layer $WS_2$ placed on a Fabry–Pérot micro-cavity (see Figure 3) [44]. The Fabry–Pérot micro-cavity facilitated strong resonant coupling between the suspended $WS_2$ and incident light, leading to a substantial enhancement and directional emission of SHG signals from $WS_2$ (Figure 3c). Furthermore, the intrinsic optical properties of 2D materials can be effectively modulated through the suspending configuration. A distinct PL was observed in suspended 2D materials compared with supported materials, as demonstrated by Luo et al. Their study on multilayer $MoS_2$ bubbles revealed simultaneous direct and indirect PL. This unique behavior was attributed to the weakening of interlayer coupling in the multilayer $MoS_2$ bubbles, as corroborated by low-frequency Raman spectroscopy [91].

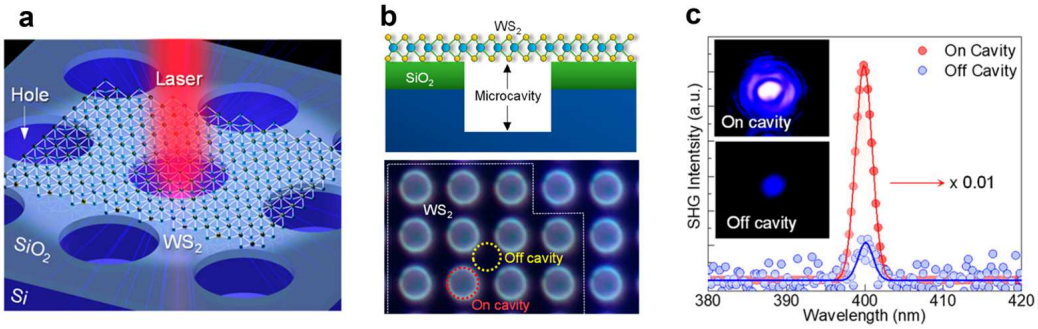


**Figure 3.** (**a**) The schematic illustrates the $WS_2$ monolayer positioned above the hole pattern on the $SiO_2$/Si substrate with laser light illuminating onto the suspended area. (**b**) Upper panel: schematic of the Fabry–Pérot microcavity composed of the $WS_2$ flake and the hole in the $SiO_2$/Si substrate. Lower panel: dark-field image of the $WS_2$ flake on the $SiO_2$/Si hole structure, where the red/yellow dashed circle represents the signals that are excited/detected on the hole area and on the substrate, which are labeled as "On cavity" and "Off cavity", respectively. The scale bar is 5 µm. (**c**) With the laser excitation at a wavelength of 800 nm, the SHG spectra and the optical image of $WS_2$ monolayer On cavity (red curve and the upper inset) and Off cavity (blue curve and the lower inset), respectively [44]. Reprinted with permission from Ref. [44]. Copyright 2022, American Physical Society.

Suspended 2D materials offer a unique opportunity to study their mechanical properties, which possess an exceptionally large surface area and an extremely thin thickness, leading to remarkable mechanical characteristics such as stiffness and elastic modulus. One article by Guo et al. employed real-space light-reflection mapping to investigate the spatially varying strain distribution in atomically thin suspended $WSe_2$ flakes (Figure 4) [118]. The suspending configuration allows for more accurate and higher-resolution measurements of strain compared with supported ones, where the substrate-induced strain obscures local strain measurements. The study, supported by their theoretical model [119], provided valuable insights into the mechanical properties of suspended 2D materials. Moreover, the suspended structure enabled the exploration of strain gradients' effects on the optical and electronic properties of $WSe_2$ flakes, leading to localized changes in the electronic bandgap. This finding holds significance for the engineering and optimization of electromechanical devices based on suspended 2D materials. In another study, Liao et al. [120] introduced a novel droplet impact method to investigate the mechanical properties of large-area suspended graphene. Using a drop impingement approach, the researchers examined the relationship between the effective Young's modulus and the thickness of suspended graphene. Precisely directed micron-sized droplets were employed via an ink-jet printing system to investigate the mechanical property. The research findings revealed a direct correlation between the Young's modulus of suspended graphene flakes and their reduced

lateral size and suspending area. These comprehensive findings, obtained through diverse experimental approaches and meticulous control over nanometer thickness, provide compelling evidence to address the ongoing debate concerning the influence of the thickness on the mechanical properties of suspended 2D materials.

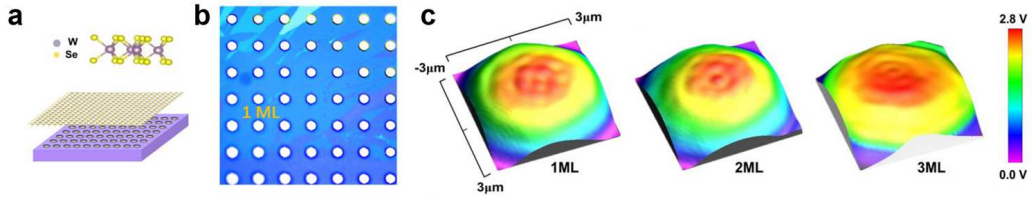


**Figure 4.** (**a**) The schematic illustrates an atomically thin $WSe_2$ flake transferred onto an array of hole structures on a $Si/SiO_2$ substrate. (**b**) Optical microscope image of monolayer $WSe_2$ on the hole substrate. (**c**) Suspended monolayer, bilayer, and tri–layer $WSe_2$ flakes are displayed in a 3D view of real-space reflection mappings [118].

Additionally, suspended 2D materials offer an excellent platform for studying the thermal expansion properties, distinguishing them from supported materials. The unique characteristic of suspended 2D materials, arising from their single-layer or few-layer atomic structure, provides higher degrees of freedom, allowing for more significant expansion or contraction along the in-plane direction without being constrained by the supporting material. Consequently, investigating and measuring the thermal expansion properties of suspended 2D materials become more accurate and straightforward. In the article by Lin et al., Raman spectroscopy measurements were employed under the condition of varying temperature (Figure 5a,b) to study the thermal response of few-layer suspended $MoS_2$. By utilizing the suspended structure of few-layer $MoS_2$, the researchers minimized the influence of substrate-induced strain, facilitating precise measurement of the thermal expansion efficiency. The findings indicate that the thermal expansion efficiency of few-layer $MoS_2$ increased proportionally with rising temperature (Figure 5c) [52]. Interestingly, the thermal expansion behavior of few-layer $MoS_2$ exhibited high anisotropy, with a significantly larger expansion coefficient perpendicular to the plane (out-of-plane) compared with the parallel direction (in-plane). This anisotropic characteristic bears relevance in developing novel strategies for engineering the thermal properties of suspended-2D-material-based devices.

Superconductivity is a highly sought-after property for electronic and quantum devices, and numerous studies have explored the potential of superconductivity in 2D materials [121–124]. In this context, suspended 2D materials offer unique advantages for investigating superconductivity due to reduced substrate-induced disorder. In this article [125], the authors utilized double-side ionic gating to induce superconductivity in suspended $MoS_2$ bilayers (Figure 6). When subjected solely to top-gating, a potent gating potential confines carriers to the uppermost layer, breaking the symmetry and leading to an accumulation of electrons in the K and K' pockets [126], resembling the band structure of a standalone monolayer. However, gating from both sides of a suspended bilayer $MoS_2$ (Figure 6a) preserved overall symmetry, resulting in the presence of charge carriers in both Q pockets and K pockets. This enabled a significantly larger number of charge carriers compared with the case where only one side was gated. By carefully tuning the ionic gate voltages, Ising pairing was induced in both the upper and lower layers of the suspended bilayer $MoS_2$, leading to an improved gate control and increased critical temperature for superconductivity. This discovery demonstrates the significant promise for the development of new 2D superconductors (Figure 6b) [127]. In another study, Mizuno et al. created suspended graphene–superconductor interfaces to investigate electron scattering and variations in electric potential caused by the contact between graphene and superconductors on conventional substrates [128]. Through this experiment, they successfully fabricated suspended monolayer graphene-NbN Josephson junctions with remarkable mobility exceeding 150,000 $cm^2/Vs$, a carrier concentration below $10^{10}$ $cm^{-2}$, and the conduction of a superconducting current at temperatures above 2 K. The devices demonstrated Joseph-

son currents influenced directly by the Fermi energy of graphene, consistent with the expected behavior based on the linear energy dispersion of Dirac electrons. This suspending approach enabled better investigation of their superconducting properties, deepening the understanding of the electronic dispersion and superconducting phase transition of 2D materials.

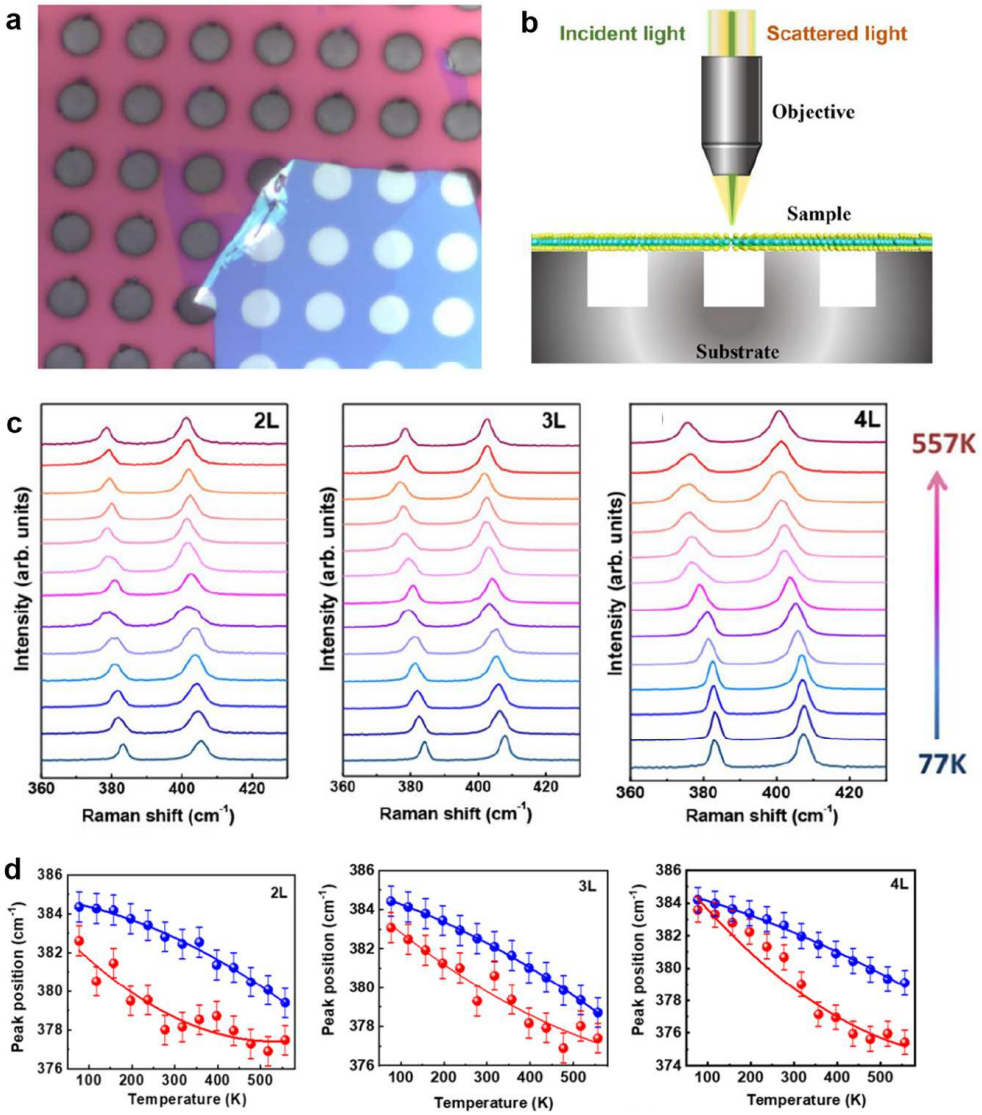


**Figure 5.** (**a**) Optical image of bilayer $MoS_2$ on a prepatterned $SiO_2$/ Si substrate with a 5 μm hole array. (**b**) The schematic diagram shows the Raman measurement setup for $MoS_2$ suspended above micro holes. (**c**) Raman spectra of suspended 2L, 3L, and 4L $MoS_2$ at different temperatures [52]. (**d**) Temperature dependence of peak positions of the $E_{2g}$ mode for the suspended and supported $MoS_2$ with different numbers of layers. The blue spheres and red spheres represent the experimental results of supported and suspended $MoS_2$, respectively. The blue lines and red lines are the fitting results obtained using a second-order polynomial function of temperature.

In summary, the suspended 2D materials show excellent properties in the electronic, mechanical, and thermal aspects, compared with the supported ones. The detailed comparisons are summarized in Table 1 (graphene) and Table 2 ($MoS_2$). The insights gained from those studies on suspended 2D materials play a crucial role in advancing our understanding of the intrinsic properties of 2D materials and furthering their applications in various fields.

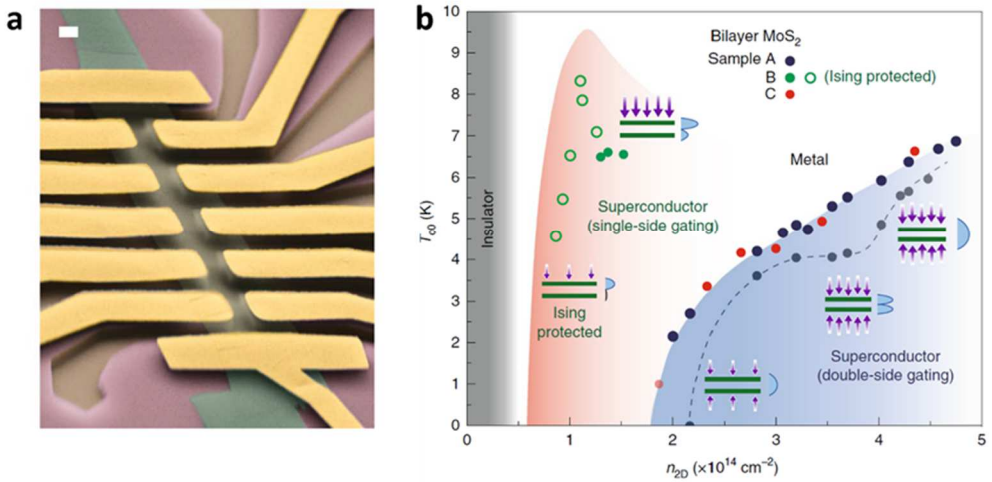


**Figure 6.** (**a**) The SEM image exhibits a representative Hall bar device of a bilayer $MoS_2$ suspended across trenches and immersed in the ionic liquid, with a scale bar of 1 μm. (**b**) The superconducting phase diagram shows the single−gated bilayer device labeled as Sample B in green and double−side gated bilayer devices represented by Samples A and C in blue and red, respectively. The red shaded region is reproduced from [127]. Reprinted with permission from Ref. [125]. Copyright 2012, AAAS.

**Table 1.** Comparison of the properties between supported graphene and suspended graphene.

| | Graphene | Suspended Graphene |
|---|---|---|
| Mobility [1] | 2000–15,000 $cm^2/Vs$ | 250,000 $cm^2/Vs$ |
| Thermal conductivity [2] | 600 W/mK | 2000–5000 W/mK |
| Tensile strains | — | 1% |

[1] The mobility of graphene was measured at a temperature of 4 K [43]. [2] The thermal conductivity of graphene was measured using Raman spectroscopy [43].

**Table 2.** Comparison of properties between supported $MoS_2$ and suspended $MoS_2$.

| | $MoS_2$ | Suspended $MoS_2$ |
|---|---|---|
| Mobility [1] | 0.1 $cm^2/Vs$ | 0.9 $cm^2/Vs$ |
| On/off ratio [1] | $10^4$ | $10^5$ |
| Young modulus [2] | — | 0.33 ± 0.07 Tpa |

[1] Electrical properties of the devices were measured in a vacuum condition ($1 \times 10^{-4}$ Torr) at room temperature [42]. [2] Young modulus was measured using atomic force microscopy (AFM) [99].

## 4. Applications of Suspended 2D Materials

Suspended 2D materials offer significant potential for a diverse range of applications due to their ultra-thin nature, high strength, high conductivity, and high transparency. One prominent application lies in electronic devices, including FETs [41,60,61], logic gates [62,63], photodetectors [64–68], resonators [69–72], and sensors [73–78]. For instance, Han et al. demonstrated that incorporating piezoresistive properties in suspended graphene membranes enhances sensitivity and expands the temperature-sensing range in nanoelectromechanical system (NEMS) temperature sensors [129]. In the case of pressure sensors, the working mechanism relies on the local compression deformation of the suspended graphene lattice. External pressure causes deformation, which alters the transport properties of electrons and, thus, changes the resistance of the sensor. Smith et al. created a suspended graphene film connected to four electrical contacts (Figure 7 illustrates the schematic of the sensor), resulting in a pressure sensor capable of detecting pressure changes with high sensitivity and stability [130]. Furthermore, Chen et al. successfully prepared ultra-large suspended graphene and employed it to fabricate capacitive pressure sensors as well, which exhibited significantly higher sensitivity compared with traditional silicon-based sensors [131]. Such pressure sensors based on suspended 2D materials hold

potential for applications in MEMS, biomedicine, and environmental monitoring. In addition to temperature and pressure sensors, suspended 2D materials have applications in optical sensors, biosensors, and chemical sensors, with the advantages of high sensitivity, stability, and fast response speed.

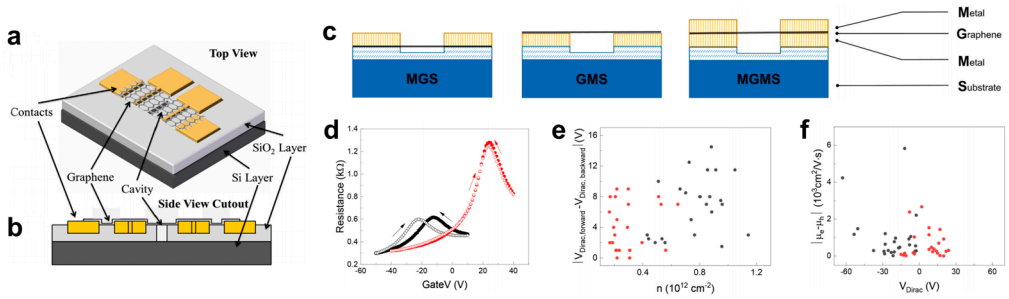


**Figure 7.** (**a**) Isometric representation of the envisioned structure of the device. (**b**) Cross−sectional view of the envisioned device structure. [130] Reprinted with permission from Ref. [130]. (**c**) Three variations of constructed device configurations for suspended graphene FETs. (**d**) With a bias voltage of 1 mV, the graph illustrates the overall resistance−gate voltage relationship. Red markers represent the suspended graphene FET, while gray markers represent the substrate–supported graphene FET. (**e**) The graph illustrates the carrier density-dependent Dirac voltage variation. (**f**) Electron mobility versus Dirac voltage. [101] Reprinted with permission from Ref. [101].

Moreover, suspended 2D materials possess high carrier mobility and low stray capacitance, making them ideal materials for FETs. Wang et al. [41] applied ionic liquid gate control to suspended $MoS_2$ FETs, resulting in significant improvements in conductivity and mobility compared with substrate-supported devices. The research findings indicate that suspended 2D materials allow for more efficient charge induction, enabling better performance as FETs. Shin et al. [101] fabricated suspended graphene FETs using the sandwich configuration (Figure 7c) and investigated their electrical properties. The suspension of the active channel (Figure 7d) in graphene FETs caused a shift of the Dirac point, a decrease in the carrier density, and an improvement in the mobility, attributed to suspended graphene devices being less affected by charged impurities on the substrate surface (Figure 7e,f). Suspended graphene FETs exhibit high carrier mobility and excellent electron–photon interaction capabilities, making them promising for high-speed circuits, optoelectronic devices, and other applications.

Resonators fabricated from suspended 2D materials offer notable advantages, particularly in terms of mass sensing capabilities and other aspects. The unique characteristics of suspended 2D materials, such as their atomic thickness and extremely low intrinsic mass, contribute to the enhanced sensitivity and resonant frequency of these resonators. In a study conducted by Jia et al. [69], large-scale arrays of suspended $MoS_2$ atomic layers were prepared to serve as nanomechanical resonators. The investigation encompassed a diverse set of $MoS_2$ nano-resonators, with structures ranging from single-layer to few-layers. The results revealed primary resonances within the high-frequency range, demonstrating an outstanding figure-of-merit of approximately $f_0 \times Q \approx 3 \times 10^{10}$ Hz. These resonators exhibited higher uniformity in terms of frequency and less energy dissipation, and they showcased reduced levels of initial tension compared with earlier findings. This pioneering research opens up new possibilities for constructing nanomechanical devices using suspended 2D materials, emphasizing the potential for highly sensitive and efficient resonator applications.

In the field of photodetection, the suspended 2D materials exhibit elevated carrier mobility, resulting in the rapid conversion of photoelectric signals and a fast response speed in photodetectors [66]. A case in point is the work of Zhong et al., wherein a suspended GaS photodetector was fabricated [68]. The findings evinced that the photodetector employing a suspended architecture showcased a remarkably fast response covering the ultraviolet to the visible spectral range. This is attributed to the suspended structure, which effectively

mitigates interface scattering and surface defects, thereby unleashing the intrinsic virtues of GaS and improving device performance. This study serves as a pivotal touchstone for the roadmap of forthcoming optoelectronic integrated devices. Furthermore, the work by Liu et al. employed a suspended $MoS_2$ photodetector (Figure 8a) through the transfer of multi-layer $MoS_2$ onto a patterned sapphire substrate (Figure 8b) [64]. Therefore, the suspended 2D materials manifest great optoelectronic characteristics in the field of photodetectors, improving the photodetection efficiency and engendering novel vistas for the evolution of optoelectronic technology.

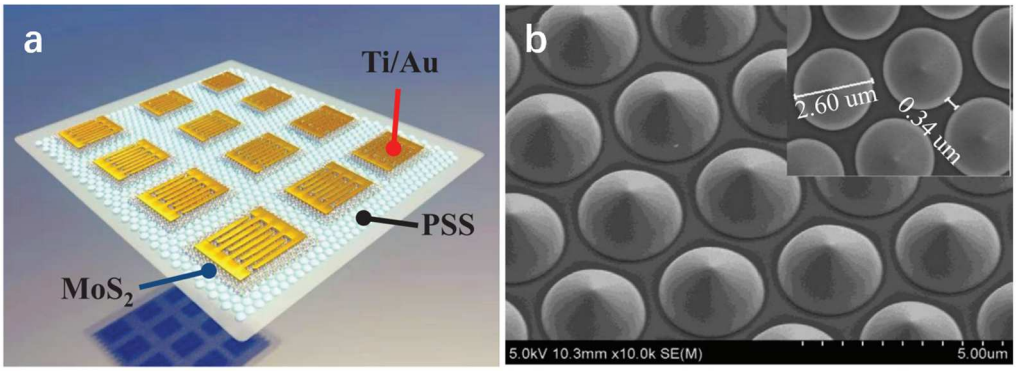


**Figure 8.** (**a**) Three-dimensional schematic diagram of $MoS_2$ photodetector based on patterned sapphire substrates. (**b**) SEM image of patterned sapphire substrates, inset describes the size of the patterned sapphire substrate array. Reprinted with permission from Ref. [64].

Additionally, suspended 2D materials exhibit great potential within the of logic gates. Wang et al. [62] introduced a plasmonic Feynman gate leveraging suspended graphene nano-ribbon waveguides. In comparison to the plasmonic Fermi gate grounded on a substrate, the plasmonic Fermi gate constructed upon a suspended architecture affords superior performance in terms of extinction ratio and crosstalk mitigation, which furnishes valuable insights in the logic circuits.

In conclusion, 2D materials possess distinctive structures and properties that render them extremely promising for a wide range of applications in the future. They hold significant importance in scientific research and engineering across multiple fields. Ongoing investigation into the properties and characteristics of 2D materials is expected to lead to further innovations and groundbreaking discoveries, paving the way for new and exciting applications.

## 5. Perspective and Conclusions

In this review, we have summarized the recent progress in the fabrication, characterization, and applications of suspended 2D materials. Although significant progress has been made in the past few years, there are still many areas that require further exploration and opportunities for future research. One key challenge is the development of new fabrication techniques that can produce large-scale suspended 2D materials with high quality and reproducibility [56,74,132]. The optimization of nanofabrication processes for suspended 2D materials can provide a great platform for future-generation optoelectronic devices. Another challenge is the development of new theoretical models that can accurately predict the electronic, optical, and mechanical properties of suspended 2D materials, taking into account the effects of strain, defects, and interactions with other materials.

On the other hand, there are also many exciting opportunities for future research on suspended 2D materials. The unique mechanical properties of suspended 2D materials make them ideal candidates for nanoelectromechanical systems (NEMS), such as resonators and sensors [133]. In addition, there is a need to explore the potential of suspended 2D materials for applications beyond electronics and photonics. For example, suspended 2D materials could be used as membranes for separation or filtration applications [134,135].

The exceptional interplay of a significant surface-to-volume relationship and mechanical flexibility in 2D materials makes them compelling candidates for such applications.

In conclusion, the progress in suspended 2D materials has been remarkable in recent years, with significant advances in fundamental understanding and technological applications. Nevertheless, there exist several challenges that must be tackled to fully unlock the potential of suspended 2D materials. Future research in this area will focus on developing reliable and scalable techniques for suspending 2D materials, understanding the effect of the suspended structure on their properties, exploring their potential for applications beyond electronics and photonics, and investigating the synergistic effects of combining different 2D materials. The insights gained from these studies could open up new avenues for developing novel materials and devices with unprecedented functionalities.

**Author Contributions:** Writing—original draft preparation, Y.D. and T.X.; writing—review and editing, Y.D., T.X., X.H. (Xinyu Huang), D.Z., J.Z., V.L., L.L., X.X. and Y.H.; visualization, X.H. (Xu Han), M.H. and J.Y.; supervision, Y.W. and Y.H.; project administration, Y.W. and Y.H.; funding acquisition, Y.D., Y.W. and Y.H. All authors have read and agreed to the published version of the manuscript.

**Funding:** This work was supported by the National Key Research and Development Program of China (Grant Nos. 2019YFA0308000, 2022YFA1403302, 2021YFA1401800, 2018YFA0704200, 2021YFA1400100, and 2020YFA0308800), the National Natural Science Foundation of China (Grant Nos. 62375020, 62022089, 11874405, 61971035, 92163206, 61888102, 52272135, and 62274010), Chongqing Outstanding Youth Fund (Grant No. 2021ZX0400005), the Beijing Natural Science Foundation (No. Z19J00015), and the Strategic Priority Research Program (B) of the Chinese Academy of Sciences (Grant No. XDB33000000).

**Acknowledgments:** The authors thank the National Key Research and Development Program of China (Grant Nos. 2019YFA0308000, 2022YFA1403302, 2021YFA1401800, 2018YFA0704200, 2021YFA1400100, and 2020YFA0308800), the National Natural Science Foundation of China (Grant Nos. 62375020, 62022089, 11874405, 61971035, 92163206, 61888102, 52272135, and 62274010), Chongqing Outstanding Youth Fund (Grant No. 2021ZX0400005), the Beijing Natural Science Foundation (No. Z19J00015), and the Strategic Priority Research Program (B) of the Chinese Academy of Sciences (Grant No. XDB33000000).

**Conflicts of Interest:** The authors declare no conflict of interest.

## References

1. Bonaccorso, F.; Sun, Z.; Hasan, T.; Ferrari, A.C. Graphene photonics and optoelectronics. *Nat. Photonics* **2010**, *4*, 611–655. [CrossRef]
2. Wang, Q.H.; Kalantar-Zadeh, K.; Kis, A.; Coleman, J.N.; Strano, M.S. Electronics and optoelectronics of two-dimensional transition metal dichalcogenides. *Nat. Nanotechnol.* **2012**, *7*, 699–712. [CrossRef] [PubMed]
3. Xu, X.D.; Yao, W.; Xiao, D.; Heinz, T.F. Spin and pseudospins in layered transition metal dichalcogenides. *Nat. Phys.* **2014**, *10*, 343–350. [CrossRef]
4. Bolotin, K.I.; Sikes, K.J.; Jiang, Z.; Klima, M.; Fudenberg, G.; Hone, J.; Kim, P.; Stormer, H.L. Ultrahigh electron mobility in suspended graphene. *Solid State Commun.* **2008**, *146*, 351–355. [CrossRef]
5. Dai, Y.Y.; Wang, Y.D.; Das, S.; Xue, H.; Bai, X.Y.; Hulkko, E.; Zhang, G.Y.; Yang, X.X.; Dai, Q.; Sun, Z.P. Electrical Control of Interband Resonant Nonlinear Optics in Monolayer $MoS_2$. *ACS Nano* **2020**, *14*, 8442–8448. [CrossRef] [PubMed]
6. Jiang, T.; Huang, D.; Cheng, J.; Fan, X.; Zhang, Z.; Shan, Y.; Yi, Y.; Dai, Y.; Shi, L.; Liu, K.; et al. Gate-tunable third-order nonlinear optical response of massless Dirac fermions in graphene. *Nat. Photonics* **2018**, *12*, 430–436. [CrossRef]
7. Chiout, A.; Brochard-Richard, C.; Marty, L.; Bendiab, N.; Zhao, M.Q.; Johnson, A.T.C.; Oehler, F.; Ouerghi, A.; Chaste, J. Extreme mechanical tunability in suspended $MoS_2$ resonator controlled by Joule heating. *npj 2D Mater. Appl.* **2023**, *7*, 20. [CrossRef]
8. Autere, A.; Jussila, H.; Dai, Y.Y.; Wang, Y.D.; Lipsanen, H.; Sun, Z.P. Nonlinear Optics with 2D Layered Materials. *Adv. Mater.* **2018**, *30*, 1465. [CrossRef]
9. Xue, H.; Wang, Y.D.; Dai, Y.Y.; Kim, W.; Jussila, H.; Qi, M.; Susoma, J.; Ren, Z.Y.; Dai, Q.; Zhao, J.L.; et al. A $MoSe_2/WSe_2$ Heterojunction-Based Photodetector at Telecommunication Wavelengths. *Adv. Funct. Mater.* **2018**, *28*, 1804388. [CrossRef]
10. Du, L.; Molas, M.R.; Huang, Z.; Zhang, G.; Wang, F.; Sun, Z. Moiré photonics and optoelectronics. *Science* **2023**, *379*, eadg0014. [CrossRef]
11. Fiori, G.; Bonaccorso, F.; Iannaccone, G.; Palacios, T.; Neumaier, D.; Seabaugh, A.; Banerjee, S.K.; Colombo, L. Electronics based on two-dimensional materials. *Nat. Nanotechnol.* **2014**, *9*, 768–779. [CrossRef] [PubMed]
12. Yang, S.X.; Chen, Y.J.; Jiang, C.B. Strain engineering of two-dimensional materials: Methods, properties, and applications. *InfoMat* **2021**, *3*, 397–420. [CrossRef]

13. Abd-Elrahim, A.G.; Chun, D.-M. Facile one-step deposition of $Co_3O_4$-$MoS_2$ nanocomposites using a vacuum kinetic spray process for non-enzymatic $H_2O_2$ sensing. *Surf. Interfaces* **2020**, *21*, 100748. [CrossRef]
14. Abd-Elrahim, A.G.; Chun, D.-M. Heterostructured $Mn_3O_4$-2D material nanosheets: One-step vacuum kinetic spray deposition and non-enzymatic $H_2O_2$ sensing. *Ceram. Int.* **2021**, *47*, 35111–35123. [CrossRef]
15. Abd-Elrahim, A.G.; Chun, D.-M. Facile one-step deposition of ZnO-graphene nanosheets hybrid photoanodes for enhanced photoelectrochemical water splitting. *J. Alloys Compd.* **2021**, *870*, 159430. [CrossRef]
16. Abd-Elrahim, A.G.; Chun, D.-M. Room-temperature deposition of ZnO-graphene nanocomposite hybrid photocatalysts for improved visible-light-driven degradation of methylene blue. *Ceram. Int.* **2021**, *47*, 12812–12825. [CrossRef]
17. Chen, X.; Yu, H.; Gao, Y.; Wang, L.; Wang, G. The marriage of two-dimensional materials and phase change materials for energy storage, conversion and applications. *EnergyChem* **2022**, *4*, 100071. [CrossRef]
18. Khan, K.; Tareen, A.K.; Aslam, M.; Zhang, Y.; Wang, R.; Ouyang, Z.; Gou, Z.; Zhang, H. Recent advances in two-dimensional materials and their nanocomposites in sustainable energy conversion applications. *Nanoscale* **2019**, *11*, 21622–21678. [CrossRef]
19. Rhodes, D.; Chae, S.H.; Ribeiro-Palau, R.; Hone, J. Disorder in van der Waals heterostructures of 2D materials. *Nat. Mater.* **2019**, *18*, 541–549. [CrossRef]
20. Zhao, T.E.; Guo, J.X.; Li, T.T.; Wang, Z.; Peng, M.; Zhong, F.; Chen, Y.; Yu, Y.Y.; Xu, T.F.; Xie, R.Z.; et al. Substrate engineering for wafer-scale two-dimensional material growth: Strategies, mechanisms, and perspectives. *Chem. Soc. Rev.* **2023**, *52*, 1650–1671. [CrossRef]
21. Chae, W.H.; Cain, J.D.; Hanson, E.D.; Murthy, A.A.; Dravid, V.P. Substrate-induced strain and charge doping in CVD-grown monolayer $MoS_2$. *Appl. Phys. Lett.* **2017**, *111*, 143106. [CrossRef]
22. Liang, J.; Zhang, J.; Li, Z.Z.; Hong, H.; Wang, J.H.; Zhang, Z.H.; Zhou, X.; Qiao, R.X.; Xu, J.Y.; Gao, P.; et al. Monitoring Local Strain Vector in Atomic-Layered $MoSe_2$ by Second-Harmonic Generation. *Nano Lett.* **2017**, *17*, 7539–7543. [CrossRef]
23. Peng, Z.W.; Chen, X.L.; Fan, Y.L.; Srolovitz, D.J.; Lei, D.Y. Strain engineering of 2D semiconductors and graphene: From strain fields to band-structure tuning and photonic applications. *Light-Sci. Appl.* **2020**, *9*, 190. [CrossRef] [PubMed]
24. Castriota, M.; Politano, G.G.; Vena, C.; De Santo, M.P.; Desiderio, G.; Davoli, M.; Cazzanelli, E.; Versace, C. Variable Angle Spectroscopic Ellipsometry investigation of CVD-grown monolayer graphene. *Appl. Surf. Sci.* **2019**, *467–468*, 213–220. [CrossRef]
25. Haidari, M.M.; Kim, H.; Kim, J.H.; Park, M.; Lee, H.; Choi, J.S. Doping effect in graphene-graphene oxide interlayer. *Sci. Rep.* **2020**, *10*, 8258. [CrossRef]
26. Politano, G.G.; Vena, C.; Desiderio, G.; Versace, C. Variable angle spectroscopic ellipsometry characterization of turbostratic CVD-grown bilayer and trilayer graphene. *Opt. Mater.* **2020**, *107*, 110165. [CrossRef]
27. Hwang, Y.; Kim, T.; Shin, N. Interlayer Energy Transfer and Photoluminescence Quenching in $MoSe_2$/Graphene van der Waals Heterostructures for Optoelectronic Devices. *ACS Appl. Nano Mater.* **2021**, *4*, 12034–12042. [CrossRef]
28. Pollmann, E.; Sleziona, S.; Foller, T.; Hagemann, U.; Gorynski, C.; Petri, O.; Madauss, L.; Breuer, L.; Schleberger, M. Large-Area, Two-Dimensional $MoS_2$ Exfoliated on Gold: Direct Experimental Access to the Metal-Semiconductor Interface. *ACS Omega* **2021**, *6*, 15929–15939. [CrossRef] [PubMed]
29. Xiao, X.; Zhang, Y.; Zhou, L.; Li, B.; Gu, L. Photoluminescence and Fluorescence Quenching of Graphene Oxide: A Review. *Nanomaterials* **2022**, *12*, 2444. [CrossRef] [PubMed]
30. Yin, H.; Hu, D.; Geng, X.; Liu, H.; Wan, Y.; Guo, Z.; Yang, P. 2D gold supercrystal-$MoS_2$ hybrids: Photoluminescence quenching. *Mater. Lett.* **2019**, *255*, 126531. [CrossRef]
31. Zhou, S.Y.; Gweon, G.H.; Fedorov, A.V.; First, P.N.; de Heer, W.A.; Lee, D.H.; Guinea, F.; Castro Neto, A.H.; Lanzara, A. Substrate-induced bandgap opening in epitaxial graphene. *Nat. Mater.* **2007**, *6*, 770–775. [CrossRef] [PubMed]
32. Huang, Y.; Wang, Y.K.; Huang, X.Y.; Zhang, G.H.; Han, X.; Yang, Y.; Gao, Y.A.; Meng, L.; Wang, Y.S.; Geng, G.Z.; et al. An efficient route to prepare suspended monolayer for feasible optical and electronic characterizations of two-dimensional materials. *InfoMat* **2022**, *4*, e12274. [CrossRef]
33. Chen, J.; Zhang, G.; Li, B.W. Substrate coupling suppresses size dependence of thermal conductivity in supported graphene. *Nanoscale* **2013**, *5*, 532–536. [CrossRef] [PubMed]
34. Du, X.; Skachko, I.; Duerr, F.; Luican, A.; Andrei, E.Y. Fractional quantum Hall effect and insulating phase of Dirac electrons in graphene. *Nature* **2009**, *462*, 192–195. [CrossRef]
35. Feldman, B.E.; Martin, J.; Yacoby, A. Broken-symmetry states and divergent resistance in suspended bilayer graphene. *Nat. Phys.* **2009**, *5*, 889–893. [CrossRef]
36. Locatelli, A.; Knox, K.R.; Cvetko, D.; Mentes, T.O.; Nino, M.A.; Wang, S.C.; Yilmaz, M.B.; Kim, P.; Osgood, R.M.; Morgante, A. Corrugation in Exfoliated Graphene: An Electron Microscopy and Diffraction Study. *ACS Nano* **2010**, *4*, 4879–4889. [CrossRef]
37. Wu, S.W.; Liu, W.T.; Liang, X.G.; Schuck, P.J.; Wang, F.; Shen, Y.R.; Salmeron, M. Hot Phonon Dynamics in Graphene. *Nano Lett.* **2012**, *12*, 5495–5499. [CrossRef]
38. Jin, W.C.; Yeh, P.C.; Zaki, N.; Zhang, D.T.; Liou, J.T.; Sadowski, J.T.; Barinov, A.; Yablonskikh, M.; Dadap, J.I.; Sutter, P.; et al. Substrate interactions with suspended and supported monolayer $MoS_2$: Angle-resolved photoemission spectroscopy. *Phys. Rev. B* **2015**, *91*, 121409. [CrossRef]
39. Dolleman, R.J.; Blanter, Y.M.; van der Zant, H.S.J.; Steeneken, P.G.; Verbiest, G.J. Phonon scattering at kinks in suspended graphene. *Phys. Rev. B* **2020**, *101*, 115411. [CrossRef]

40. Hu, H.; Yu, R.W.; Teng, H.C.; Hu, D.B.; Chen, N.; Qu, Y.P.; Yang, X.X.; Chen, X.Z.; McLeod, A.S.; Alonso-Gonzalez, P.; et al. Active control of micrometer plasmon propagation in suspended graphene. *Nat. Commun.* **2022**, *13*, 1465. [CrossRef]
41. Wang, F.L.; Stepanov, P.; Gray, M.; Lau, C.N.; Itkis, M.E.; Haddon, R.C. Ionic Liquid Gating of Suspended $MoS_2$ Field Effect Transistor Devices. *Nano Lett.* **2015**, *15*, 5284–5288. [CrossRef] [PubMed]
42. Jin, T.; Kang, J.; Su Kim, E.; Lee, S.; Lee, C. Suspended single-layer $MoS_2$ devices. *J. Appl. Phys.* **2013**, *114*, 164509. [CrossRef]
43. Lau, C.N.; Bao, W.; Velasco, J. Properties of suspended graphene membranes. *Mater. Today* **2012**, *15*, 238–245. [CrossRef]
44. Shi, J.; Wu, X.; Wu, K.; Zhang, S.; Sui, X.; Du, W.; Yue, S.; Liang, Y.; Jiang, C.; Wang, Z.; et al. Giant Enhancement and Directional Second Harmonic Emission from Monolayer $WS_2$ on Silicon Substrate via Fabry-Pérot Micro-Cavity. *ACS Nano* **2022**, *16*, 13933–13941. [CrossRef]
45. Liu, L.; Gong, P.; Liu, K.; Nie, A.; Liu, Z.; Yang, S.; Xu, Y.; Liu, T.; Zhao, Y.; Huang, L.; et al. Scalable Van der Waals Encapsulation by Inorganic Molecular Crystals. *Adv. Mater.* **2022**, *34*, e2106041. [CrossRef] [PubMed]
46. Sattari-Esfahlan, S.M.; Kim, H.G.; Hyun, S.H.; Choi, J.H.; Hwang, H.S.; Kim, E.T.; Park, H.G.; Lee, J.H. Low-Temperature Direct Growth of Amorphous Boron Nitride Films for High-Performance Nanoelectronic Device Applications. *ACS Appl. Mater. Interfaces* **2023**, *15*, 7274–7281. [CrossRef] [PubMed]
47. Tan, C.; Jiang, J.; Wang, J.; Yu, M.; Tu, T.; Gao, X.; Tang, J.; Zhang, C.; Zhang, Y.; Zhou, X.; et al. Strain-Free Layered Semiconductors for 2D Transistors with On-State Current Density Exceeding 1.3 mA $um^{-1}$. *Nano Lett.* **2022**, *22*, 3770–3776. [CrossRef] [PubMed]
48. Vu, Q.A.; Fan, S.; Lee, S.H.; Joo, M.-K.; Yu, W.J.; Lee, Y.H. Near-zero hysteresis and near-ideal subthreshold swing in h-BN encapsulated single-layer $MoS_2$ field-effect transistors. *2D Mater.* **2018**, *5*, 031001. [CrossRef]
49. Ahmed, Z.; Afzalian, A.; Schram, T.; Jang, D.; Verreck, D.; Smets, Q.; Schuddinck, P.; Chehab, B.; Sutar, S.; Arutchelvan, G.; et al. Introducing 2D-FETs in Device Scaling Roadmap using DTCO. In Proceedings of the 2020 IEEE International Electron Devices Meeting (IEDM), San Francisco, CA, USA, 12–18 December 2020.
50. Huang, Y.; Pan, Y.H.; Yang, R.; Bao, L.H.; Meng, L.; Luo, H.L.; Cai, Y.Q.; Liu, G.D.; Zhao, W.J.; Zhou, Z.; et al. Universal mechanical exfoliation of large-area 2D crystals. *Nat. Commun.* **2020**, *11*, 2453. [CrossRef]
51. Huang, X.Y.; Zhang, L.; Liu, L.W.; Qin, Y.; Fu, Q.; Wu, Q.; Yang, R.; Lv, J.P.; Ni, Z.H.; Liu, L.; et al. Raman spectra evidence for the covalent-like quasi-bonding between exfoliated $MoS_2$ and Au films. *Sci. China-Inf. Sci.* **2021**, *64*, 140406. [CrossRef]
52. Lin, Z.; Liu, W.; Tian, S.; Zhu, K.; Huang, Y.; Yang, Y. Thermal expansion coefficient of few-layer $MoS_2$ studied by temperature-dependent Raman spectroscopy. *Sci. Rep.* **2021**, *11*, 7037. [CrossRef] [PubMed]
53. Liu, X.S.; Jin, J.Y.; Liu, J.; Sun, L.F.; Yang, C.C.; Li, Y.J. Molten liquid metal motion assisted preparation of suspended graphene arrays. *Mater. Lett.* **2022**, *314*, 131874. [CrossRef]
54. Meyer, J.C.; Geim, A.K.; Katsnelson, M.I.; Novoselov, K.S.; Booth, T.J.; Roth, S. The structure of suspended graphene sheets. *Nature* **2007**, *446*, 60–63. [CrossRef] [PubMed]
55. Ci, H.N.; Chen, J.T.; Ma, H.; Sun, X.L.; Jiang, X.Y.; Liu, K.C.; Shan, J.Y.; Lian, X.Y.; Jiang, B.; Liu, R.J.; et al. Transfer-Free Quasi-Suspended Graphene Grown on a Si Wafer. *Adv. Mater.* **2022**, *34*, 2206389. [CrossRef] [PubMed]
56. Suzuki, H.; Kaneko, T.; Shibuta, Y.; Ohno, M.; Maekawa, Y.; Kato, T. Wafer-scale fabrication and growth dynamics of suspended graphene nanoribbon arrays. *Nat. Commun.* **2016**, *7*, 11797. [CrossRef] [PubMed]
57. Hamer, M.J.; Hopkinson, D.G.; Clark, N.; Zhou, M.W.; Wang, W.D.; Zou, Y.C.; Kelly, D.J.; Bointon, T.H.; Haigh, S.J.; Gorbachev, R.V. Atomic Resolution Imaging of $CrBr_3$ Using Adhesion-Enhanced Grids. *Nano Lett.* **2020**, *20*, 6582–6589. [CrossRef] [PubMed]
58. Chaste, J.; Hnid, I.; Khalil, L.; Si, C.; Durnez, A.; Lafosse, X.; Zhao, M.Q.; Johnson, A.T.C.; Zhang, S.B.; Bang, J.; et al. Phase Transition in a Memristive Suspended $MoS_2$ Monolayer Probed by Opto- and Electro-Mechanics. *ACS Nano* **2020**, *14*, 13611–13618. [CrossRef]
59. Dai, C.H.; Rho, Y.; Pham, K.; McCormick, B.; Blankenship, B.W.; Zhao, W.Y.; Zhang, Z.C.; Crommie, M.F.; Wang, F.; Grigoropoulos, C.P.; et al. Kirigami Engineering of Suspended Graphene Transducers. *Nano Lett.* **2022**, *22*, 5301–5306. [CrossRef] [PubMed]
60. Choi, W.R.; Hong, J.H.; You, Y.G.; Campbell, E.E.B.; Jhang, S.H. Suspended $MoTe_2$ field effect transistors with ionic liquid gate. *Appl. Phys. Lett.* **2021**, *119*, 223105. [CrossRef]
61. Chen, H.; Li, J.; Chen, X.; Zhang, D.; Zhou, P. Dramatic switching behavior in suspended $MoS_2$ field-effect transistors. *Semicond. Sci. Technol.* **2018**, *33*, 024001. [CrossRef]
62. Wang, P.J.; Ding, J.; Chen, W.W.; Li, S.Q.; Zhang, B.H.; Lu, H.; Li, J.; Li, Y.; Fu, Q.; Dai, T.G.; et al. Plasmonic Feynman Gate Based on Suspended Graphene Nano-Ribbon Waveguides at THz Wavelengths. *IEEE Photonics J.* **2019**, *11*, 4801109. [CrossRef]
63. Safinezhad, A.; Eslami, M.R.; Jafari Jozani, K.; Rezaei, M.H. Ultra-compact all-optical reversible Feynman gate based on suspended graphene plasmonic waveguides. *Opt. Quantum Electron.* **2022**, *54*, 295. [CrossRef]
64. Liu, X.; Hu, S.; Luo, J.; Li, X.; Wu, J.; Chi, D.; Ang, K.W.; Yu, W.; Cai, Y. Suspended $MoS_2$ Photodetector Using Patterned Sapphire Substrate. *Small* **2021**, *17*, e2100246. [CrossRef] [PubMed]
65. Liu, Y.; Jiang, Y.; Tan, C.; Li, Y.; Chen, Y.; Li, Z.; Gao, L.; Yang, L.; Wang, Z. Strain Tune Suspended $MoS_2$ for Polarization Photodetection. *Phys. Status Solidi (RRL) Rapid Res. Lett.* **2023**, 2300101. [CrossRef]
66. Saenz, G.A.; Karapetrov, G.; Curtis, J.; Kaul, A.B. Ultra-high Photoresponsivity in Suspended Metal-Semiconductor-Metal Mesoscopic Multilayer $MoS_2$ Broadband Detector from UV-to-IR with Low Schottky Barrier Contacts. *Sci. Rep.* **2018**, *8*, 1276. [CrossRef]

67. Thakar, K.; Mukherjee, B.; Grover, S.; Kaushik, N.; Deshmukh, M.; Lodha, S. Multilayer $ReS_2$ Photodetectors with Gate Tunability for High Responsivity and High-Speed Applications. *ACS Appl. Mater. Interfaces* **2018**, *10*, 36512–36522. [CrossRef]
68. Zhong, W.; Liu, Y.; Yang, X.; Wang, C.; Xin, W.; Li, Y.; Liu, W.; Xu, H. Suspended few-layer GaS photodetector with sensitive fast response. *Mater. Des.* **2021**, *212*, 110233. [CrossRef]
69. Jia, H.; Yang, R.; Nguyen, A.E.; Alvillar, S.N.; Empante, T.; Bartelsb, L.; Feng, P.X.L. Large-scale arrays of single- and few-layer $MoS_2$ nanomechanical resonators. *Nanoscale* **2016**, *8*, 10677–10685. [CrossRef] [PubMed]
70. Song, X.; Oksanen, M.; Sillanpaa, M.A.; Craighead, H.G.; Parpia, J.M.; Hakonen, P.J. Stamp transferred suspended graphene mechanical resonators for radio frequency electrical readout. *Nano Lett.* **2012**, *12*, 198–202. [CrossRef]
71. Jung, M.; Rickhaus, P.; Zihlmann, S.; Eichler, A.; Makk, P.; Schonenberger, C. GHz nanomechanical resonator in an ultraclean suspended graphene p-n junction. *Nanoscale* **2019**, *11*, 4355–4361. [CrossRef]
72. Singh, V.; Irfan, B.; Subramanian, G.; Solanki, H.S.; Sengupta, S.; Dubey, S.; Kumar, A.; Ramakrishnan, S.; Deshmukh, M.M. Coupling between quantum Hall state and electromechanics in suspended graphene resonator. *Appl. Phys. Lett.* **2012**, *100*, 233103. [CrossRef]
73. Zhang, B.; Li, Q.; Cui, T.H. Ultra-sensitive suspended graphene nanocomposite cancer sensors with strong suppression of electrical noise. *Biosens. Bioelectron.* **2012**, *31*, 105–109. [CrossRef] [PubMed]
74. Lemme, M.C.; Wagner, S.; Lee, K.; Fan, X.; Verbiest, G.J.; Wittmann, S.; Lukas, S.; Dolleman, R.J.; Niklaus, F.; van der Zant, H.S.J.; et al. Nanoelectromechanical Sensors Based on Suspended 2D Materials. *Research* **2020**, *2020*, 8748602. [CrossRef] [PubMed]
75. Masurkar, N.; Varma, S.; Mohana Reddy Arava, L. Supported and Suspended 2D Material-Based FET Biosensors. *Electrochem* **2020**, *1*, 260–277. [CrossRef]
76. Suzuki, D.; Li, K.; Ishibashi, K.; Kawano, Y. A Terahertz Video Camera Patch Sheet with an Adjustable Design based on Self-Aligned, 2D, Suspended Sensor Array Patterning. *Adv. Funct. Mater.* **2021**, *31*, 2008931. [CrossRef]
77. Gupta, R.K.; Alqahtani, F.H.; Dawood, O.M.; Carini, M.; Criado, A.; Prato, M.; Garlapati, S.K.; Jones, G.; Sexton, J.; Persaud, K.C.; et al. Suspended graphene arrays for gas sensing applications. *2D Mater.* **2020**, *8*, 025006. [CrossRef]
78. Regmi, A.; Shin, D.; Kim, J.-H.; Choi, S.; Chang, J. Suspended graphene sensor with controllable width and electrical tunability via direct-write functional fibers. *J. Manuf. Process.* **2020**, *58*, 458–465. [CrossRef]
79. Wang, Q.; Lei, Y.; Wang, Y.; Liu, Y.; Song, C.; Zeng, J.; Song, Y.; Duan, X.; Wang, D.; Li, Y. Atomic-scale engineering of chemical-vapor-deposition-grown 2D transition metal dichalcogenides for electrocatalysis. *Energy Environ. Sci.* **2020**, *13*, 1593–1616. [CrossRef]
80. Hu, C.X.; Shin, Y.; Read, O.; Casiraghi, C. Dispersant-assisted liquid-phase exfoliation of 2D materials beyond graphene. *Nanoscale* **2021**, *13*, 460–484. [CrossRef] [PubMed]
81. Hoang, A.T.; Qu, K.; Chen, X.; Ahn, J.H. Large-area synthesis of transition metal dichalcogenides via CVD and solution-based approaches and their device applications. *Nanoscale* **2021**, *13*, 615–633. [CrossRef]
82. Liu, J.P.; Liu, H.B.; Peng, W.C.; Li, Y.; Zhang, F.B.; Fan, X.B. High-yield exfoliation of $MoS_2$ ($WS_2$) monolayers towards efficient photocatalytic hydrogen evolution. *Chem. Eng. J.* **2022**, *431*, 133286. [CrossRef]
83. Zhu, W.S.; Gao, X.; Li, Q.; Li, H.P.; Chao, Y.H.; Li, M.J.; Mahurin, S.M.; Li, H.M.; Zhu, H.Y.; Dai, S. Controlled Gas Exfoliation of Boron Nitride into Few-Layered Nanosheets. *Angew. Chem. Int. Ed.* **2016**, *55*, 10766–10770. [CrossRef] [PubMed]
84. Abd-Elrahim, A.G.; Chun, D.-M. Kinetically induced one-step heterostructure formation of $Co_3O_4$-$Ni(OH)_2$-graphene ternary nanocomposites to enhance oxygen evolution reactions. *J. Alloys Compd.* **2022**, *906*, 164159. [CrossRef]
85. Abdolhosseinzadeh, S.; Zhang, C.J.; Schneider, R.; Shakoorioskooie, M.; Nuesch, F.; Heier, J. A Universal Approach for Room-Temperature Printing and Coating of 2D Materials. *Adv. Mater.* **2022**, *34*, e2103660. [CrossRef]
86. Moses, O.A.; Gao, L.; Zhao, H.; Wang, Z.; Lawan Adam, M.; Sun, Z.; Liu, K.; Wang, J.; Lu, Y.; Yin, Z.; et al. 2D materials inks toward smart flexible electronics. *Mater. Today* **2021**, *50*, 116–148. [CrossRef]
87. Lindvall, N.; Sun, J.; Yurgens, A. Transfer-free fabrication of suspended graphene grown by chemical vapor deposition. In Proceedings of the 2012 7th IEEE International Conference on Nano/Micro Engineered and Molecular Systems (NEMS), Kyoto, Japan, 5–8 March 2012; pp. 19–22.
88. Huang, Y.; Sutter, E.; Shi, N.N.; Zheng, J.B.; Yang, T.Z.; Englund, D.; Gao, H.J.; Sutter, P. Reliable Exfoliation of Large-Area High-Quality Flakes of Graphene and Other Two-Dimensional Materials. *ACS Nano* **2015**, *9*, 10612–10620. [CrossRef]
89. Velicky, M.; Donnelly, G.E.; Hendren, W.R.; McFarland, S.; Scullion, D.; DeBenedetti, W.J.I.; Correa, G.C.; Han, Y.M.; Wain, A.J.; Hines, M.A.; et al. Mechanism of Gold-Assisted Exfoliation of Centimeter-Sized Transition-Metal Dichalcogenide Monolayers. *ACS Nano* **2018**, *12*, 10463–10472. [CrossRef]
90. Liu, F.; Wu, W.J.; Bai, Y.S.; Chae, S.H.; Li, Q.Y.; Wang, J.; Hone, J.; Zhu, X.Y. Disassembling 2D van der Waals crystals into macroscopic monolayers and reassembling into artificial lattices. *Science* **2020**, *367*, 903–906. [CrossRef]
91. Luo, H.L.; Li, X.Y.; Zhao, Y.C.; Yang, R.; Bao, L.H.; Hao, Y.F.; Gao, Y.N.; Shi, N.N.; Guo, Y.; Liu, G.D.; et al. Simultaneous generation of direct- and indirect-gap photoluminescence in multilayer $MoS_2$ bubbles. *Phys. Rev. Mater.* **2020**, *4*, 074006. [CrossRef]
92. Lloyd, D.; Liu, X.H.; Boddeti, N.; Cantley, L.; Long, R.; Dunn, M.L.; Bunch, J.S. Adhesion, Stiffness, and Instability in Atomically Thin $MoS_2$ Bubbles. *Nano Lett.* **2017**, *17*, 5329–5334. [CrossRef]
93. Stolyarova, E.; Stolyarov, D.; Bolotin, K.; Ryu, S.; Liu, L.; Rim, K.T.; Klima, M.; Hybertsen, M.; Pogorelsky, I.; Pavlishin, I.; et al. Observation of Graphene Bubbles and Effective Mass Transport under Graphene Films. *Nano Lett.* **2009**, *9*, 332–337. [CrossRef] [PubMed]

94. Villarreal, R.; Lin, P.C.; Faraji, F.; Hassani, N.; Bana, H.; Zarkua, Z.; Nair, M.N.; Tsai, H.C.; Auge, M.; Junge, F.; et al. Breakdown of Universal Scaling for Nanometer-Sized Bubbles in Graphene. *Nano Lett.* **2021**, *21*, 8103–8110. [CrossRef] [PubMed]
95. Prydatko, A.V.; Belyaeva, L.A.; Jiang, L.; Lima, L.M.C.; Schneider, G.F. Contact angle measurement of free-standing square-millimeter single-layer graphene. *Nat. Commun.* **2018**, *9*, 4185. [CrossRef]
96. Yue, K.; Gao, W.; Huang, R.; Liechti, K.M. Analytical methods for the mechanics of graphene bubbles. *J. Appl. Phys.* **2012**, *112*, 083512. [CrossRef]
97. Bertolazzi, S.; Brivio, J.; Kis, A. Stretching and Breaking of Ultrathin $MoS_2$. *ACS Nano* **2011**, *5*, 9703–9709. [CrossRef] [PubMed]
98. Castellanos-Gomez, A.; Poot, M.; Steele, G.A.; van der Zant, H.S.J.; Agrait, N.; Rubio-Bollinger, G. Elastic Properties of Freely Suspended $MoS_2$ Nanosheets. *Adv. Mater.* **2012**, *24*, 772–775. [CrossRef]
99. Huang, J.Y.; Qi, L.; Li, J. In situ imaging of layer-by-layer sublimation of suspended graphene. *Nano Res.* **2010**, *3*, 43–50. [CrossRef]
100. Sharbidre, R.S.; Byen, J.C.; Yun, G.Y.; Ryu, J.K.; Lee, C.J.; Hong, S.G.; Bramhe, S.; Kim, T.N. Residue Free Fabrication of Suspended 2D Nanosheets for in-situ TEM Nanomechanics. *Kor. J. Mater. Res.* **2018**, *28*, 627–632. [CrossRef]
101. Shin, H.; Lee, S.B. Fabrication of suspended graphene field-effect transistors by the sandwich method. *Curr. Appl. Phys.* **2023**, *48*, 42–46. [CrossRef]
102. Lemme, M.C.; Bell, D.C.; Williams, J.R.; Stern, L.A.; Baugher, B.W.H.; Jarillo-Herrero, P.; Marcus, C.M. Etching of Graphene Devices with a Helium Ion Beam. *ACS Nano* **2009**, *3*, 2674–2676. [CrossRef]
103. Nagyte, V.; Kelly, D.J.; Felten, A.; Picardi, G.; Shin, Y.Y.; Alieva, A.; Worsley, R.E.; Parvez, K.; Dehm, S.; Krupke, R.; et al. Raman Fingerprints of Graphene Produced by Anodic Electrochemical Exfoliation. *Nano Lett.* **2020**, *20*, 3411–3419. [CrossRef] [PubMed]
104. Alem, N.; Erni, R.; Kisielowski, C.; Rossell, M.D.; Gannett, W.; Zettl, A. Atomically thin hexagonal boron nitride probed by ultrahigh-resolution transmission electron microscopy. *Phys. Rev. B* **2009**, *80*, 155425. [CrossRef]
105. Archanjo, B.S.; Barboza, A.P.M.; Neves, B.R.A.; Malard, L.M.; Ferreira, E.H.M.; Brant, J.C.; Alves, E.S.; Plentz, F.; Carozo, V.; Fragneaud, B.; et al. The use of a Ga+ focused ion beam to modify graphene for device applications. *Nanotechnology* **2012**, *23*, 255305. [CrossRef]
106. Sepioni, M.; Nair, R.R.; Rablen, S.; Narayanan, J.; Tuna, F.; Winpenny, R.; Geim, A.K.; Grigorieva, I.V. Limits on Intrinsic Magnetism in Graphene. *Phys. Rev. Lett.* **2010**, *105*, 207205. [CrossRef] [PubMed]
107. Bolotin, K.I.; Sikes, K.J.; Hone, J.; Stormer, H.L.; Kim, P. Temperature-Dependent Transport in Suspended Graphene. *Phys. Rev. Lett.* **2008**, *101*, 096802. [CrossRef]
108. Deng, B.; Pang, Z.Q.; Chen, S.L.; Li, X.; Meng, C.X.; Li, J.Y.; Liu, M.X.; Wu, J.X.; Qi, Y.; Dang, W.H.; et al. Wrinkle-Free Single-Crystal Graphene Wafer Grown on Strain-Engineered Substrates. *ACS Nano* **2017**, *11*, 12337–12345. [CrossRef]
109. Mayorov, A.S.; Elias, D.C.; Mukhin, I.S.; Morozov, S.V.; Ponomarenko, L.A.; Novoselov, K.S.; Geim, A.K.; Gorbachev, R.V. How Close Can One Approach the Dirac Point in Graphene Experimentally? *Nano Lett.* **2012**, *12*, 4629–4634. [CrossRef] [PubMed]
110. Mun, J.H.; Cho, B.J. Synthesis of Monolayer Graphene Having a Negligible Amount of Wrinkles by Stress Relaxation. *Nano Lett.* **2013**, *13*, 2496–2499. [CrossRef] [PubMed]
111. Mun, J.H.; Oh, J.G.; Bong, J.H.; Xu, H.; Loh, K.P.; Cho, B.J. Wrinkle-free graphene with spatially uniform electrical properties grown on hot-pressed copper. *Nano Res.* **2015**, *8*, 1075–1080. [CrossRef]
112. Shi, Y.M.; Dong, X.C.; Chen, P.; Wang, J.L.; Li, L.J. Effective doping of single-layer graphene from underlying $SiO_2$ substrates. *Phys. Rev. B* **2009**, *79*, 115402. [CrossRef]
113. Chen, J.H.; Jang, C.; Xiao, S.D.; Ishigami, M.; Fuhrer, M.S. Intrinsic and extrinsic performance limits of graphene devices on SiO2. *Nat. Nanotechnol.* **2008**, *3*, 206–209. [CrossRef]
114. Li, Q.A.; Cheng, Z.G.; Li, Z.J.; Wang, Z.H.; Fang, Y. Fabrication of suspended graphene devices and their electronic properties. *Chin. Phys. B* **2010**, *19*, 4.
115. Feldman, B.E.; Krauss, B.; Smet, J.H.; Yacoby, A. Unconventional Sequence of Fractional Quantum Hall States in Suspended Graphene. *Science* **2012**, *337*, 1196–1199. [CrossRef] [PubMed]
116. Ki, D.K.; Fal'ko, V.I.; Abanin, D.A.; Morpurgo, A.F. Observation of Even Denominator Fractional Quantum Hall Effect in Suspended Bilayer Graphene. *Nano Lett.* **2014**, *14*, 2135–2139. [CrossRef]
117. Ki, D.K.; Morpurgo, A.F. High-Quality Multiterminal Suspended Graphene Devices. *Nano Lett.* **2013**, *13*, 5165–5170. [CrossRef]
118. Guo, Y.; Huang, Y.; Du, S.; Sun, C.; Tian, S.; Luo, H.; Liu, B.; Zhou, X.; Li, J.; Gu, C. Real-space light-reflection mapping of atomically thin $WSe_2$ flakes revealing the gradient local strain. *Mater. Res. Express* **2020**, *7*, 035904. [CrossRef]
119. Rostami, H.; Roldán, R.; Cappelluti, E.; Asgari, R.; Guinea, F. Theory of strain in single-layer transition metal dichalcogenides. *Phys. Rev. B* **2015**, *92*, 195402. [CrossRef]
120. Liao, Y.T.; Peng, S.Y.; Chuang, K.W.; Liao, Y.C.; Kuramitsu, Y.; Woon, W.Y. Exploring the mechanical properties of nanometer-thick elastic films through micro-drop impinging on large-area suspended graphene. *Nanoscale* **2021**, *14*, 42–48. [CrossRef]
121. Yoshida, M.; Kudo, K.; Nohara, M.; Iwasa, Y. Metastable Superconductivity in Two-Dimensional $IrTe_2$ Crystals. *Nano Lett.* **2018**, *18*, 3113–3117. [CrossRef]
122. Lu, J.M.; Zheliuk, O.; Leermakers, I.; Yuan, N.F.Q.; Zeitler, U.; Law, K.T.; Ye, J.T. Evidence for two-dimensional Ising superconductivity in gated $MoS_2$. *Science* **2015**, *350*, 1353–1357. [CrossRef] [PubMed]
123. Wu, F.; MacDonald, A.H.; Martin, I. Theory of Phonon-Mediated Superconductivity in Twisted Bilayer Graphene. *Phys. Rev. Lett.* **2018**, *121*, 257001. [CrossRef]

124. Potirniche, I.-D.; Maciejko, J.; Nandkishore, R.; Sondhi, S.L. Superconductivity of disordered Dirac fermions in graphene. *Phys. Rev. B* **2014**, *90*, 094516. [CrossRef]
125. Zheliuk, O.; Lu, J.M.; Chen, Q.H.; Yumin, A.A.E.; Golightly, S.; Ye, J.T. Josephson coupled Ising pairing induced in suspended $MoS_2$ bilayers by double-side ionic gating. *Nat. Nanotechnol.* **2019**, *14*, 1123–1128. [CrossRef] [PubMed]
126. Brumme, T.; Calandra, M.; Mauri, F. First-principles theory of field-effect doping in transition-metal dichalcogenides: Structural properties, electronic structure, Hall coefficient, and electrical conductivity. *Phys. Rev. B* **2015**, *91*, 155436. [CrossRef]
127. Ye, J.T.; Zhang, Y.J.; Akashi, R.; Bahramy, M.S.; Arita, R.; Iwasa, Y. Superconducting Dome in a Gate-Tuned Band Insulator. *Science* **2012**, *338*, 1193–1196. [CrossRef]
128. Mizuno, N.; Nielsen, B.; Du, X. Ballistic-like supercurrent in suspended graphene Josephson weak links. *Nat. Commun.* **2013**, *4*, 2716. [CrossRef]
129. Han, S.Q.; Zhou, S.Y.; Mei, L.Y.; Guo, M.L.; Zhang, H.Y.; Li, Q.N.; Zhang, S.; Niu, Y.K.; Zhuang, Y.; Geng, W.P.; et al. Nanoelectromechanical Temperature Sensor Based on Piezoresistive Properties of Suspended Graphene Film. *Nanomaterials* **2023**, *13*, 1103. [CrossRef]
130. Smith, A.D.; Vaziri, S.; Niklaus, F.; Fischer, A.C.; Sterner, M.; Delin, A.; Östling, M.; Lemme, M.C. Pressure sensors based on suspended graphene membranes. *Solid-State Electron.* **2013**, *88*, 89–94. [CrossRef]
131. Chen, Y.M.; He, S.M.; Huang, C.H.; Huang, C.C.; Shih, W.P.; Chu, C.L.; Kong, J.; Li, J.; Su, C.Y. Ultra-large suspended graphene as a highly elastic membrane for capacitive pressure sensors. *Nanoscale* **2016**, *8*, 3555–3564. [CrossRef] [PubMed]
132. Kim, S.-M.; Lee, C.-K.; Yoon, S.-U.; Kim, K.-S.; Hwangbo, Y. Residue-free suspended graphene transferred by perforated template. *Nanotechnology* **2022**, *33*, 165301. [CrossRef]
133. Fan, X.; Smith, A.D.; Forsberg, F.; Wagner, S.; Schröder, S.; Akbari, S.S.A.; Fischer, A.C.; Villanueva, L.G.; Östling, M.; Lemme, M.C.; et al. Manufacture and characterization of graphene membranes with suspended silicon proof masses for MEMS and NEMS applications. *Microsyst. Nanoeng.* **2020**, *6*, 17. [CrossRef] [PubMed]
134. Surwade, S.P.; Smirnov, S.N.; Vlassiouk, I.V.; Unocic, R.R.; Veith, G.M.; Dai, S.; Mahurin, S.M. Water desalination using nanoporous single-layer graphene. *Nat. Nanotechnol.* **2015**, *10*, 459–464. [CrossRef] [PubMed]
135. Yoon, H.W.; Cho, Y.H.; Park, H.B. Graphene-based membranes: Status and prospects. *Philos. Trans. R. Soc. A-Math. Phys. Eng. Sci.* **2016**, *374*, 20150024. [CrossRef] [PubMed]